

1-1-2009

Magnetic and Transport Properties of $\text{Co}_2\text{MnSn}_x\text{Sb}_{1-x}$ Heusler Alloys

Moti R. Paudel

Southern Illinois University Carbondale

Christopher S. Wolfe

Southern Illinois University Carbondale

Heather M. A. Patton

Southern Illinois University Carbondale

Igor Dubenko

Southern Illinois University Carbondale

Naushad Ali

Southern Illinois University Carbondale

See next page for additional authors

Follow this and additional works at: http://opensiuc.lib.siu.edu/phys_pubs

© 2009 American Institute of Physics

Published in *Journal of Applied Physics*, Vol. 105 No. 1 (2009) at doi: [10.1063/1.3054291](https://doi.org/10.1063/1.3054291)

Recommended Citation

Paudel, Moti R.; Christopher S. Wolfe; Heather M. A. Patton; Igor Dubenko; Naushad Ali; Joseph A. Christodoulides; and Shane Stadler. "Magnetic and Transport Properties of $\text{Co}_2\text{MnSn}_x\text{Sb}_{1-x}$ Heusler Alloys." (Jan 2009).

This Article is brought to you for free and open access by the Department of Physics at OpenSIUC. It has been accepted for inclusion in Publications by an authorized administrator of OpenSIUC. For more information, please contact opensiuc@lib.siu.edu.

Authors

Moti R. Paudel, Christopher S. Wolfe, Heather M. A. Patton, Igor Dubenko, Naushad Ali, Joseph A. Christodoulides, and Shane Stadler

Magnetic and transport properties of $\text{Co}_2\text{MnSn}_x\text{Sb}_{1-x}$ Heusler alloys

Moti R. Paudel,^{1,a)} Christopher S. Wolfe,¹ Heather Patton,¹ Igor Dubenko,¹ Naushad Ali,¹ Joseph A. Christodoulides,² and Shane Stadler^{1,b)}

¹Department of Physics, Southern Illinois University, Neckers 483 A, Carbondale, Illinois 62901, USA

²Naval Research Laboratory, Code 6360, 4555 Overlook Avenue SW, Washington, DC 20375-5320, USA

(Received 21 July 2008; accepted 11 November 2008; published online 15 January 2009)

We present the magnetic, structural, and transport properties of the quaternary Heusler alloys $\text{Co}_2\text{MnSn}_x\text{Sb}_{1-x}$ ($x=0, 0.25, 0.50, 0.75,$ and 1.0), which have been theoretically predicted to be half-metallic. Magnetization measurements as a function of applied field show that the saturation moment for $x=1$ (Co_2MnSn) is near the Slater–Pauling value of $5\mu_B$; however, the moment for $x=0$ (Co_2MnSb) falls far short of its predicted value of $6\mu_B$. Resistivity as a function of temperature was measured from 5 to 400 K, and a phase transition from a half-metallic ferromagnetic phase to a normal ferromagnetic phase was observed between 50 and 80 K for all of the alloys. At low temperature ($10\text{ K} < T < 40\text{ K}$), the resistivity ratio was found to vary as $R(T)/R(T=5\text{ K})=A+BT^2+CT^{9/2}$, where the T^2 term results from electron-electron scattering, whereas the $T^{9/2}$ term is a consequence of double magnon scattering. © 2009 American Institute of Physics.

[DOI: [10.1063/1.3054291](https://doi.org/10.1063/1.3054291)]

I. INTRODUCTION

Half-metallic, ferromagnetic Heusler alloys have been intensively studied for more than a decade due to their possible applications in the field of spintronics.¹ In half-metallic materials, one spin band possesses a metallic character while the other one is semiconducting. Ideal half-metals (100% spin polarized) thus require a band gap across the Fermi level in the minority band. There is a particular interest in the use of these alloys in spin injection, giant magnetoresistance, and tunneling magnetoresistance devices, as well as in magnetic random access memory elements.^{1–4}

The first theoretically predicted half-metal was the half-Heusler ($C1_b$) alloy NiMnSb .⁴ Full-Heusler alloys (X_2YZ) crystallize in the $L2_1$ structure, which is constructed from four interpenetrating fcc sublattices.⁵ Many stoichiometric manganese-based full-Heusler alloys such as Co_2MnSi and Co_2MnGe have been theoretically predicted to be half-metallic.^{5–7} They have high Curie temperatures, large magnetic moments, and gaps in the minority density of states (DOS), which are desirable properties for spintronics applications.^{6,8} However, due to the presence of antisite disorder, in addition to many other possible defects in real materials, there is the appearance of minority spin states at the Fermi level, which effectively destroys the predicted spin polarization.^{9–12} Following the band structure calculations of Ishida *et al.*,⁶ Co_2MnSb and Co_2MnSn are not 100% spin polarized but their mixed alloys, $\text{Co}_2\text{MnSn}_x\text{Sb}_{1-x}$ for the range of $0.2 < x < 0.6$, are predicted to be half-metallic. To the best of our knowledge, this series of compounds has found a little attention in the experimental literature. In this paper, we present the structural, magnetic, and transport

properties of these bulk compounds in order to explore their potential use for future applications in the field of spintronics.

II. EXPERIMENT

Polycrystalline bulk ($\sim 5\text{ g}$) buttons of $\text{Co}_2\text{MnSn}_x\text{Sb}_{1-x}$ alloys were fabricated using conventional arc melting procedures in an argon atmosphere using commercially available elements with $4N$ purity. The elements were melted three times and the weight loss after melting was found to be less than 0.2%. To enhance the homogeneity, they were wrapped in tantalum foil and annealed in vacuum ($< 10^{-4}$ Torr) at $850\text{ }^\circ\text{C}$ for 24 h.

Structural phases were identified through x-ray diffraction (XRD) measurements at room temperature using a GBC MMA x-ray diffractometer in Bragg–Brentano geometry using $\text{Cu K}\alpha$ radiation. The XRD scans were indexed using POWDERCELL™ commercial software.¹³ The compositional analysis was done with Rutherford backscattering (RBS) and was further confirmed using inductively coupled plasma (ICP) spectroscopy measurements. The magnetization data were acquired using a superconducting quantum interference device magnetometer manufactured by Quantum Design, Inc. and dc resistivity measurements were made using the same instrument over a temperature range of 5–400 K.

III. RESULTS AND DISCUSSION

The room temperature XRD patterns of $\text{Co}_2\text{MnSn}_x\text{Sb}_{1-x}$ ($x=0, 0.25, 0.5, 0.75,$ and 1) are shown in Fig. 1. Analyses of these XRD patterns indicate that all the samples studied are composed of a single phase except in the case of Co_2MnSb (and to a lesser degree in $\text{Co}_2\text{MnSn}_{0.25}\text{Sb}_{0.75}$), where additional, low intensity peaks were observed. These peaks could be due to the presence of a small amount of a MnSb phase, which is reinforced by the following. First, Webster⁸ reported the presence of two phases ($\text{Co}_{1.5}\text{MnSb}$ and Co) in the case

^{a)}Author to whom correspondence should be addressed. Electronic mail: paudel@siu.edu.

^{b)}Present address: Department of Physics and Astronomy, Louisiana State University, Baton Rouge, LA 70802, USA.

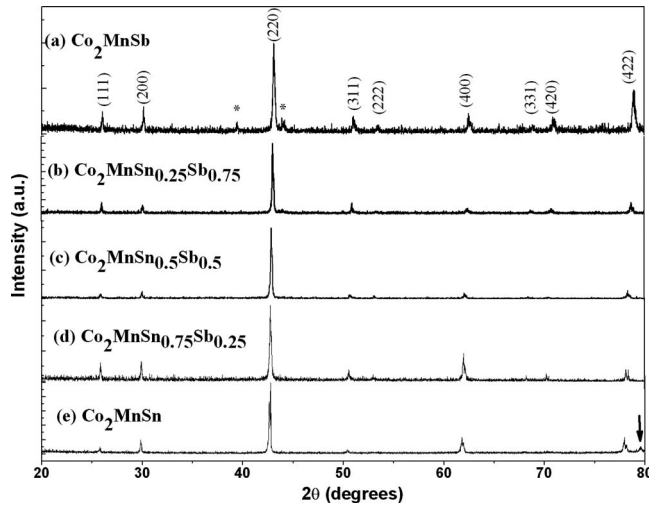


FIG. 1. Room temperature powder XRD patterns of the $\text{Co}_2\text{MnSn}_x\text{Sb}_{1-x}$ system. In part (a), the asterisks (*) indicate possible MnSb peaks. The arrow in part (e) indicates the sample holder peak (Al alloy).

of bulk Co_2MnSb , and the value of the lattice parameter for $\text{Co}_{1.5}\text{MnSb}$ was found to be 5.92 \AA . Second, Ksenofontov *et al.*¹⁴ showed through electronic structure calculations that MnSb inclusions are energetically preferable with respect to the growth of pure Co_2MnSb .

The XRD patterns were indexed according to a full-Heusler $L2_1$ cubic structure. Figure 2 shows the variation in lattice parameter with Sn concentration. Table I shows the values of the lattice parameter for all the alloys. The lattice parameters were found to increase from 5.943 \AA ($x=0$) to 6.003 \AA ($x=1$). The value of the lattice parameter for $x=1$ (Co_2MnSn) is consistent with other published results⁸ within experimental error, while there are no known published data for other compositions before this study. The increase in the lattice parameter is most likely due to the larger ionic radius of Sn (1.40 \AA) compared to that of Sb (1.36 \AA). From the variation in the lattice parameter (a) with Sn concentration (x), we see that the lattice constant increases linearly up to $x=0.5$ and then more slowly after that up to $x=1$. This behavior might be attributed to many things in the variation in the Fermi level due to a change in the DOS.

RBS measurements were done on $\text{Co}_2\text{MnSn}_x\text{Sb}_{1-x}$ and the results showed that they were very close to the nominal values. The results of the ICP measurements also indicate that both methods yield similar results for the composition within the experimental error. The results of both measurements are shown in Table I.

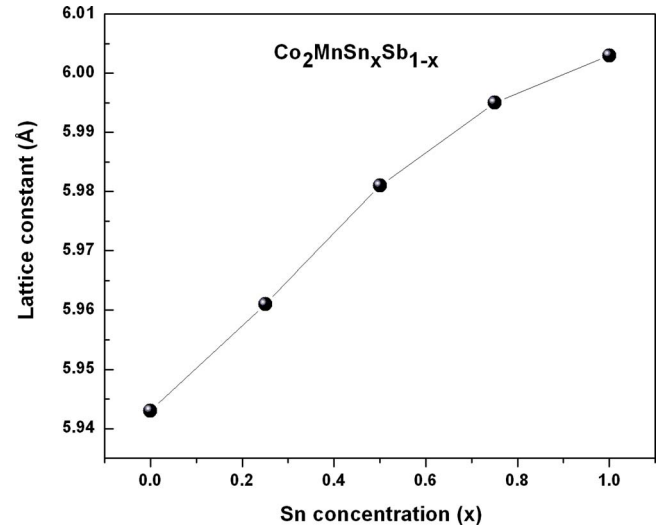


FIG. 2. (Color online) The variation in lattice constant of $\text{Co}_2\text{MnSn}_x\text{Sb}_{1-x}$ as a function of Sn concentration (x).

The magnetization (M) curves as a function of field (H) for polycrystalline $\text{Co}_2\text{MnSn}_x\text{Sb}_{1-x}$ alloys at 5 K are shown in Fig. 3. All of the magnetization curves were measured at fields ranging from 0–50 kOe. The alloys under study were found to be in the ferromagnetic phase from $T=5$ to 400 K. These alloys are magnetically soft and are nearly saturated at $H=15$ kOe. The values of the saturation magnetizations at 5 K were obtained by extrapolating the graphs of M versus $(1/H)$ to zero. The extrapolated values were then used to calculate the saturation magnetic moments (M_S) in Bohr magnetons (μ_B) per formula unit. Table I shows the calculated values of the saturation magnetic moment (M_S) for each alloy. Since there are no published results for the saturation moments of this system (except for Co_2MnSn), we cannot make direct comparisons to other studies. However, for Co_2MnSn , the reported experimental results of M_S vary from 4.78 to $5.12\mu_B$ per formula unit, and our result of $4.94\mu_B$ lies even closer to the Slater–Pauling value of $5\mu_B$.¹⁵ For Co_2MnSb , our result of $5.09\mu_B$ is far below the Slater–Pauling value of $6\mu_B$.¹⁶ This discrepancy could be due to the presence of an additional phase (such as MnSb inclusions as suggested earlier) or as a result of disorder or defects in the crystal structure.¹⁴ However, another study needs to be conducted in order to determine the origin of this behavior.

Figure 3 shows the variation in M_S with Sn concentration [inset (a)] and the lattice constant [inset (b)]. The mo-

TABLE I. Structural and magnetic parameters along with the composition analysis of the $\text{Co}_2\text{MnSn}_x\text{Sb}_{1-x}$ Heusler alloy system.

Nominal composition	Measured composition	Lattice parameter (\AA)	M_S (emu/g) at 5 K	M_S (μ_B /f.u.)
Co_2MnSb	$\text{Co}_{1.98}\text{Mn}_{1.01}\text{Sb}_{1.01}$ ^a $\text{Co}_{1.94}\text{Mn}_{1.02}\text{Sb}_{1.04}$ ^b	5.943	96.25	5.09
$\text{Co}_2\text{MnSn}_{0.25}\text{Sb}_{0.75}$...	5.962	97.65	5.13
$\text{Co}_2\text{MnSn}_{0.5}\text{Sb}_{0.5}$	$\text{Co}_{2.00}\text{Mn}_{1.01}\text{Sn}_{0.49}\text{Sb}_{0.50}$ ^a	5.981	100.23	5.26
$\text{Co}_2\text{MnSn}_{0.75}\text{Sb}_{0.25}$	$\text{Co}_{1.96}\text{Mn}_{1.01}\text{Sn}_{0.78}\text{Sb}_{0.25}$ ^b	5.995	95.98	5.06
Co_2MnSn	$\text{Co}_{2.03}\text{Mn}_{1.00}\text{Sn}_{0.97}$ ^a	6.003	94.83	4.94

^aRBS measurements.

^bICP measurements.

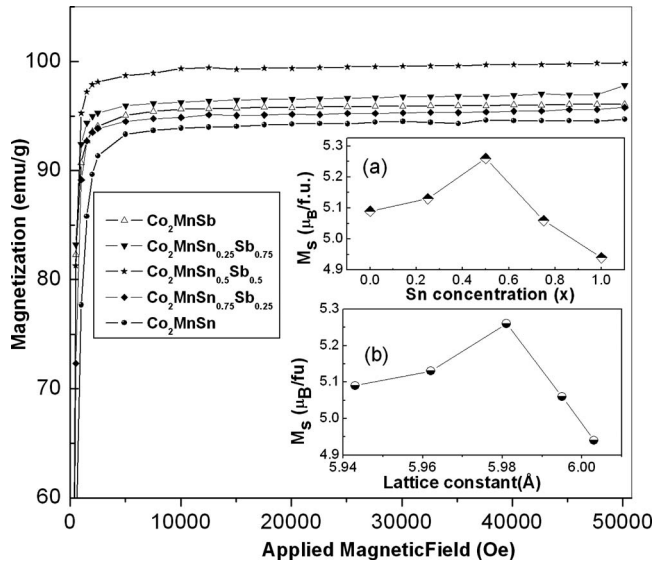


FIG. 3. The variation in magnetization of the $\text{Co}_2\text{MnSn}_x\text{Sb}_{1-x}$ system with applied magnetic field at $T=5$ K. [Inset (a)] The variation in the saturation magnetization per formula unit with lattice constant; [Inset (b)] The variation in the same with Sn concentration (x).

ment increases with increasing concentration up to $x=0.5$ and then decreases with further increase in x up to 1.0 (Co_2MnSn). The main contribution to the magnetic moment in these types of Heusler compounds comes from indirect exchange interactions between magnetic ions, and the largest fraction of the total moment originates from Mn. There is a change in the separation between magnetic ions due to the change in lattice parameter, and therefore the variation in magnetization could be attributed to a change in moment due to a Ruderman–Kittel–Kasuya–Yoshida type of coupling. A shift in the Fermi level by sp -element (Sb and Sn) substitution, along with a change in the band structure due to the change in interatomic spacing and elemental substitution, could be other reasons responsible for this behavior.

The resistance (R) curves as a function of temperature for Co_2MnSb in the range of 5–400 K for zero and 50 kOe applied fields are shown in Fig. 4. For temperatures below ~ 10 K, there is a rapid decrease in resistance with a decrease in temperature, instead of a smooth approach to the residual resistance, and this behavior disappears when the resistance is measured in the presence of an applied magnetic field. This behavior is displayed more clearly in inset (b) of Fig. 4. This could be a field-dependent structural transition that occurs at very low temperatures, but this is not presently clear. Similar behavior was observed for all of the alloys of the $\text{Co}_2\text{MnSn}_x\text{Sb}_{1-x}$ system that were studied (Fig. 5). Moreover, in Co_2MnSb at $T=5$ K, the resistance of the sample increases with the increase in applied field and is saturated at $H=50$ kOe [Fig. 4, inset (a)]. The origin of this positive magnetoresistance is not understood yet.

Omitting this low temperature behavior at $T < 10$ K, there are three regions where the resistance follows different power laws. The ratio of the resistances at a given temperature and at $T=5$ K [$R(T)/R(5\text{ K})$], which is equivalent to the corresponding resistivity ratio, is shown in Fig. 5 for all of the samples. Taking the first derivative of these curves, we

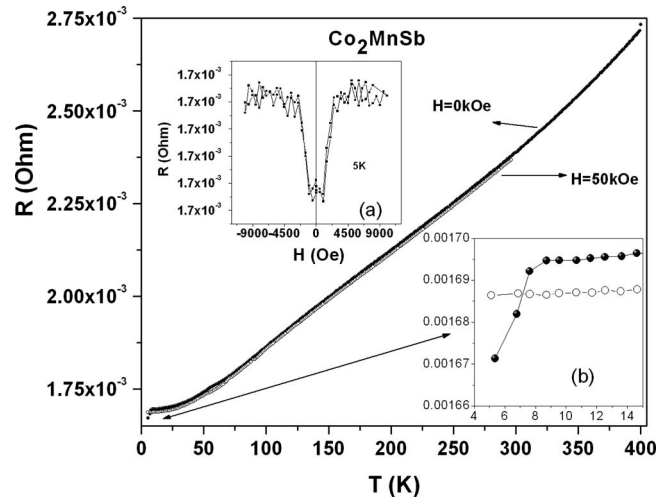


FIG. 4. The variation in the resistance of Co_2MnSb with temperature at zero and 50 kOe applied fields. [Inset (a)] The variation in resistance with applied field at 5 K; [Inset (b)] The magnetic field dependence of the resistance at low temperatures (< 10 K) shows the suppression of the transition upon the application of field.

have identified three distinct regions as stated above. In $\text{Co}_2\text{MnSn}_{0.25}\text{Sb}_{0.75}$, the resistance ratio [$R(T)/R(5\text{ K})$] is almost independent of temperature in the temperature range (9–22 K). Similar behavior is observed in the same temperature region in the case of single crystals of Co_2MnSi .¹⁷

Above this temperature, for this particular sample and for all others, there is change in temperature dependence of the resistivity, i.e., a transition that occurs at a temperature between 50 and 80 K. This transition could be a transition from a half-metallic state to a normal ferromagnetic state, similar to that observed in NiMnSb by Hordequin *et al.*¹⁸ The slope of these curves becomes almost constant after 80 K up to about 250 K. At higher temperatures (250–400 K), [$R(T)/R(5\text{ K})$] follows yet another law, as described below.

In a half-metallic system, low temperature electron scattering processes include a dominant “double magnon” scat-

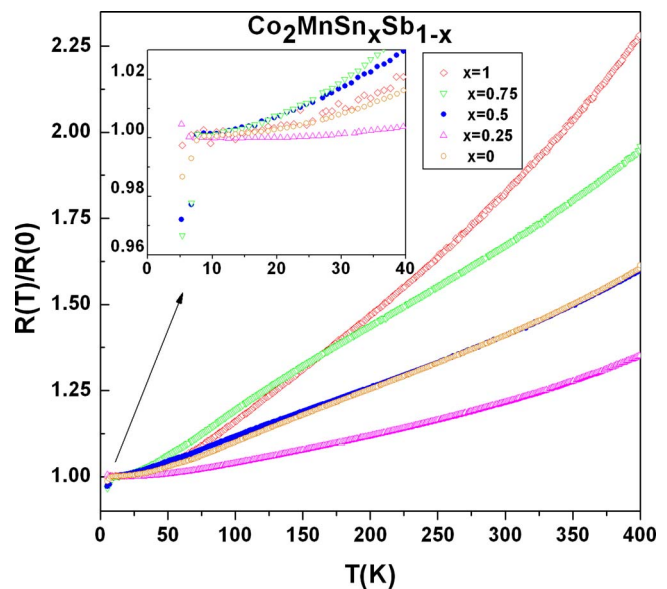


FIG. 5. (Color online) The variation in resistance of $\text{Co}_2\text{MnSn}_x\text{Sb}_{1-x}$ with temperature at zero applied field for $x=0, 0.25, 0.5, 0.75,$ and 1.

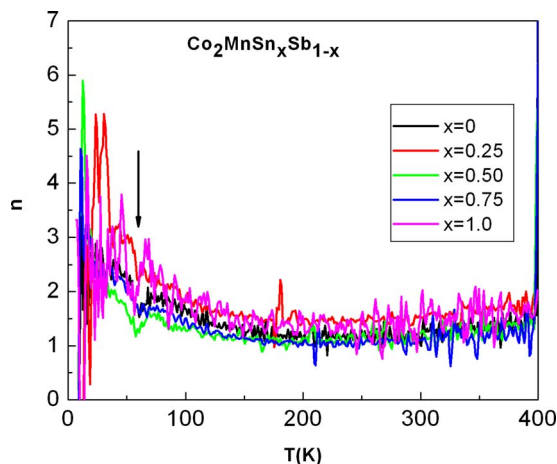


FIG. 6. (Color online) The variation in n in the power law for the resistance ($R(T)=R(0)+cT^n$) as a function of temperature for $\text{Co}_2\text{MnSn}_x\text{Sb}_{1-x}$ at zero applied field. The arrow in the figure indicates the temperature region where a phase transition occurs, which may be an evidence for a transition from a half-metallic to a normal ferromagnetic state.

tering process that has a $T^{9/2}$ dependence on the resistivity and an electron-electron scattering process which has T^2 dependence. Single magnon scattering is not possible for true half metals due to the absence of electrons in the minority band gap at the Fermi level.^{19,20} To see the relative contributions of these two scattering processes, we have fitted the resistivity ratio of the $\text{Co}_2\text{MnSn}_x\text{Sb}_{1-x}$ alloys as $R(T)/R(5\text{ K})=A+BT^2+CT^{9/2}$. For each concentration of x studied, this power law fits well up to 40 K. We have calculated the relative contributions of the T^2 and $T^{9/2}$ behaviors in the total resistivity ratio within the temperature range studied. In all cases, the T^2 contribution is dominant up to 20 K, while $T^{9/2}$ is dominant above 20 up to 40 K. Thus we can conclude that the scattering processes are due to electron-electron scattering and double magnon scattering in this Heusler system in the low temperature range.

To compare the power laws in different temperature regions with other studies, we have fitted the resistivity data to the power law $R(T)/R(5\text{ K})=a+bT^n$ for all of the alloys. Figure 6 shows the variation in the power (n) as a function of temperature. From Fig. 6, we see that the value of n varies from 1.25 to 1.8 in the higher temperature region (250–400 K). In the middle temperature region (100–250 K), the value of n varies from 1.0 to 1.45. For temperatures of <50 K, the average value of n is 2.5 for all the samples except $x=0.25$, which has an average value of $n=4.25$. In Co_2MnGe single crystal films, Ambrose *et al.*²¹ reported $n=1.5$ in the high temperature region ($50 < T < 400$) K.

The room temperature resistivity ratios (RRRs) [$R(300)/R(5\text{ K})$] for $\text{Co}_2\text{MnSn}_x\text{Sb}_{1-x}$ vary from 1.22 for $x=0.25$ to 1.82 for $x=1$. For all other alloys studied the ratio is around 1.5. These values are smaller than the previously reported value (2.92) in single crystalline¹⁷ as well as (2.7) in arc-melted¹¹ Co_2MnSi . The smaller values are likely due to the specific crystalline quality of the alloys used in this study, i.e., to the presence of lattice defects and other forms of disorder. Moreover, most of them are quaternary rather than ternary alloys. The deviation of $R(T)$ from a linear dependence with temperature (for a pure phonon contribution in

the scattering process) at higher temperatures also indicates that there are defects and disorder in the crystals. However, the highest RRR was 1.82, as observed in Co_2MnSn .

In conclusion, we fabricated the bulk alloys $\text{Co}_2\text{MnSn}_x\text{Sb}_{1-x}$ using arc melting methods and studied their structural, magnetic, and transport properties. For $x=0$ and 0.25, there was a small contribution of a second phase (probably a MnSb phase) in addition to the dominant $L2_1$ Heusler phase. For all other alloys, the phase was pure Heusler $L2_1$. The saturation magnetization for $x=0$ (Co_2MnSb) was found to be much lower than the Slater–Pauling value of $6\mu_B$, which could be due to the presence of a second phase or to imperfections and disorder in the crystal structure. For $x=1$ (Co_2MnSn), the saturation magnetization was close to the previously reported value as well as to the Slater–Pauling value of $5\mu_B$. At low temperatures (<40 K), both electron-electron scattering and double magnon scattering were responsible for the observed transport behavior. At temperatures less than 10 K, a sharp magnetic-field-dependent change in the resistance was observed, the origin of which is not known. A phase transition was observed between 50 and 80 K that, as identified in other works on half-Heusler alloys, could be an evidence of a transition from a half-metallic to a normal ferromagnetic state.

ACKNOWLEDGMENTS

This work is supported by the National Science Foundation (CAREER Grant No. NSF-DMR-0545728).

- ¹G. A. Prinz, *Science* **282**, 1660 (1998); *Phys. Today* **48**, 58 (1995).
- ²W. A. Pickett and J. S. Moodera, *Phys. Today* **54**, 39 (2001).
- ³J. M. Kikkawa and D. D. Awschalom, *Nature (London)* **397**, 139 (1999).
- ⁴R. A. de Groot, F. M. Mueller, P. G. van Engen, and K. H. J. Buschow, *Phys. Rev. Lett.* **50**, 2024 (1983).
- ⁵S. Ishida, T. Masaki, S. Fujii, and S. Asano, *Physica B* **245**, 1 (1998).
- ⁶S. Ishida, S. Fuji, S. Kashiwagi, and S. Asano, *J. Phys. Soc. Jpn.* **64**, 2152 (1995).
- ⁷I. Galanakis, P. H. Dederichs, and N. Papanikolaou, *Phys. Rev. B* **66**, 174429 (2002).
- ⁸P. J. Webster, *J. Phys. Chem. Solids* **32**, 1221 (1971).
- ⁹S. Picozzi, A. Continenza, and A. J. Freeman, *Phys. Rev. B* **69**, 094423 (2004).
- ¹⁰S. Picozzi, A. Continenza, and A. J. Freeman, *J. Magn. Magn. Mater.* **272–276**, 315 (2004).
- ¹¹M. P. Raphael, B. Ravel, Q. Huang, M. A. Willard, S. F. Cheng, B. N. Das, R. M. Stroud, K. M. Bussmann, J. H. Claassen, and V. G. Harris, *Phys. Rev. B* **66**, 104429 (2002).
- ¹²B. Ravel, J. O. Cross, M. P. Raphael, V. G. Harris, R. Ramesh, and V. Saraf, *Appl. Phys. Lett.* **81**, 2812 (2002).
- ¹³W. Kraus and G. Nolze, *J. Appl. Crystallogr.* **29**, 301 (1996).
- ¹⁴V. Ksenofontov, G. Melnyk, M. Wojcik, S. Wurmehl, K. Kroth, S. Riemann, P. Blaha, and C. Felser, *Phys. Rev. B* **74**, 134426 (2006).
- ¹⁵P. J. Brown, K. U. Neumann, P. J. Webster, and K. R. A. Ziebeck, *J. Phys.: Condens. Matter* **12**, 1827 (2000).
- ¹⁶I. Galanakis and P. Mavropoulos, *J. Phys.: Condens. Matter* **19**, 315213 (2007).
- ¹⁷L. Ritchie, G. Xiao, Y. Ji, T. Y. Chen, C. L. Chien, M. Zhang, J. Chen, Z. Liu, G. Wu, and X. X. Zhang, *Phys. Rev. B* **68**, 104430 (2003).
- ¹⁸C. Hordequin, D. Ristiou, L. Ranno, and J. Pierre, *Eur. Phys. J. B* **16**, 287 (2000).
- ¹⁹K. Kubo and N. Ohata, *J. Phys. Soc. Jpn.* **33**, 21 (1972).
- ²⁰J. M. Zimen, *Electrons and Phonons* (Oxford University Press, London, 1967).
- ²¹T. Ambrose, J. J. Krebs, and G. A. Prinz, *Appl. Phys. Lett.* **76**, 3280 (2000).